Fish and Shellfish Immunology 84 (2019) 673–679

Contents lists available at ScienceDirect

Fish and Shellfish Immunology

journal homepage: www.elsevier.com/locate/fsi

Full length article

Expression profiling and microbial ligand binding analysis of galectin-4 in turbot (*Scophthalmus maximus* L.)

Jinghua Chen[1], Lu Zhang[1], Ning Yang, Mengyu Tian, Qiang Fu, Fenghua Tan, Chao Li*

Marine Science and Engineering College, Qingdao Agricultural University, Qingdao, 266109, People's Republic of China

ARTICLE INFO

Keywords:
Galectin-4
Turbot
Vibrio anguillarum
Streptococcus iniae
Microbial ligand binding

ABSTRACT

Galectins are a family of galactoside-binding proteins with an affinity for β-galactosides, involved in mediating fundamental processes including development, inflammation, cell migration and apoptosis. Galectin-4 is a member of tendem-repeat galectins, plays vital roles in intestinal epithelial barrier. Here, one galectin-4 gene was captured in turbot (*Sm*Lgals4) contains a 1197 bp open reading frame (ORF). In comparison to other species, *Sm*Lgals4 showed the highest similarity and identity both to large yellow croaker. The genomic structure analysis showed that *Sm*Lgals4 had conserved exons in the CRD domains compared to other vertebrate species. The syntenic analysis revealed that galectin-4 had the same neighboring genes across all the selected species, which suggested the synteny encompassing galectin-4 region during vertebrate evolution. Subsequently, *Sm*Lgals4 was widely expressed in all the examined tissues, with the highest expression level in intestine and the lowest expression level in skin. In addition, *Sm*Lgals4 was significantly down-regulated in intestine following both Gram-negative bacteria *Vibrio anguillarum*, and Gram-positive bacteria *Streptococcus iniae* immersion challenge. Finally, the *rSm*Lgals4 showed strong binding ability to all the examined microbial ligands. Taken together, our results suggested *Sm*Lgals4 plays vital roles in fish intestinal immune responses against infection, but the detailed roles of galectin-4 in teleost are still lacking, further studies are needed to be carried out to characterize whether galectin-4 plays similar roles in teleost intestinal immunity.

1. Introduction

As living in the pathogen-rich aquatic environment, the immune system plays more important roles for teleost species than mammals against a wide range of pathogens in external environment [1]. The first step of innate immune responses is the pathogen recognition, which depends on pathogen recognition receptors (PRRs). During pathogen attachment and entry, the PRRs could recognize the pathogen associated molecular patterns (PAMP) including lipopolysaccharide (LPS), peptidoglycan (PGN), glucan, and mannan presenting on the surface of microbes, and triggering the downstream immune signaling pathways to eliminate the pathogens [2]. Lectins are a group of sugar-binding proteins that recognize specific carbohydrate structures in the pathogen membranes, that involved in pathogen recognition as pivotal components of innate immune response [3,4]. Lectins present in almost all the living organisms, and could be divided into C-type lectins, galectins, F-type lectins, rhamnose-binding lectins, and intelectins [5].

Among the lectin families, galectins are a family of galactoside-binding proteins with an affinity for β-galactosides, involved in mediating fundamental processes including development, inflammation, cell migration and apoptosis [6,7]. The galectin family has been classified into three different types: proto-type, chimera type and tandem-repeat type [8]. Prototype galectins include galectin-1, -2, -7, -10, −13 and −14, usually homodimers of non-covalently linked subunits. Tandem-repeat galectins include galectin-4, -6, -8, -9, and -12, usually monomeric with two CRDs joined together by a linker peptide [8]. However, chimera type galectins are monomeric which two carbohydrate-recognition domains (CRD-I on the N-terminal and CRD-II on the C-terminal sides) joined by a linker peptide, and only composed by galectin-4 [9]. Galectin-4 was originally identified in rat intestinal extracts in 1989 as a soluble lectin [10]. Since then, more and more studies have revealed its vital roles in intestinal epithelial barrier in mammals. For instance, it has been reported to be involved in postnatal development of small intestine [11], intestinal epithelial wound wealing [12], and intestinal inflammation [13,14]. In teleost, galectin-4 showed strong bactericidal activity in *Channa striatus* [15]. Although the function of galectin-4 has been well documented in mammals, the studies of galectin-4 are still limited in teleost.

* Corresponding author.
E-mail address: leoochao@163.com (C. Li).
[1] All these authors contributed equally to this work.

https://doi.org/10.1016/j.fsi.2018.10.050
Received 8 August 2018; Received in revised form 10 October 2018; Accepted 20 October 2018
Available online 22 October 2018
1050-4648/

Turbot (*Scophthalmus maximus* L.), one of the most extensively maricultured species in China, suffers from the bacterial disease including *Vibrio anguillarum* and *Streptococcus iniae*. Especially, the teleost mucosal surfaces (skin, gill and intestine) are constantly colonized with various pathogens presenting in the aquatic environment [16]. Therefore, characterization of mucosal immune-related genes as well as associated activities during pathogen infection could expand our knowledge of the teleost immunity, and move forward to develop disease control strategies via immersion or feeding [17]. In turbot, many studies have been performed to identify the immune-related genes and investigate their associated activities during bacterial infection [18–22]. In this regard, with the vital roles of galectin-4 in mucosal barriers, we sought here to identify galectin-4 in turbot, as well as its expression patterns following different bacterial infection, and microbial ligand-binding activities.

2. Materials and methods

2.1. Sequence identification and analysis

In order to capture galectin-4 gene in turbot (*Sm*Lgals4), the protein sequences of other species were collected as queries to BLAST against turbot databases [23,24]. The retrieved candidate sequences were then translated using ORF Finder (http://www.ncbi.nlm.nih.gov/gorf/gorf.html). The predicted ORF sequences were further verified against NCBI non-redundant protein sequence database by BLASTP (http://blast.ncbi.nlm.nih.gov/Blast.cgi). The theoretical pI, molecular mass and N-glycosylation sites were characterized in ExPASy server [25]. The intron and exon structures were predicted by Splign program [26]. The identity and similarity among the different species of galectin-4 gene were calculated using MatGAT program [27].

2.2. Phylogenetic analysis

The phylogenetic tree was constructed based on the amino acids sequences of galectin-4 genes from various species including human (*Homo sapiens*), mouse (*Mus musculus*), frog (*Xenopus tropicalis*), central bearded dragon (*Pogona vitticeps*), bald eagle (*Haliaeetus leucocephalus*), mexican tetra (*Astyanax mexicanus*), *Ictalurus punctatus* (channel catfish), Japanese medaka (*Oryzias latipes*), half-smooth tongue sole (*Cynoglossus semilaevis*), large yellow croaker (*Larimichthys crocea*), and turbot. The multiple sequence alignment was performed in Clustal Omega program [28]. Molecular Evolutionary Genetics Analysis package (MEGA 6) was utilized to construct neighbor-joining phylogenetic tree [29].

2.3. Syntenic analysis

In order to further verify the identification of *Sm*Lgals4, the syntenic analysis was performed across several species. Briefly, the protein sequences of neighboring genes of the *Sm*Lgals4 were predicted from the turbot scaffold using FGENESH program. The identified protein sequences were annotated by BLASTP program against NCBI non-redundant (nr) database. The conserved syntenic pattern of galectin-4 gene in other species were characterized in Ensembl database and Genomicus [30].

2.4. Bacteria challenge and sample collection

We further investigated the expression profiles of *Sm*Lgals4 following Gram-negative bacteria *V. anguillarum* and Gram-positive bacteria *S. iniae* bath challenge in turbot mucosal tissues (skin, gill and intestine). Turbot fingerlings (average body weight: 15.6 g and average body length = 5.5 cm) were obtained from the turbot hatchery (Haiyang, Shandong, China), and acclimated in the laboratory in a flow-through system for at least two weeks prior to challenge. After a pre-challenge, the bacteria was re-isolated from single symptomatic fish and biochemically confirmed before cultured. At each timepoint following challenge, skin, gill and intestine samples were collected from 15 fish (5 fish per pool) from the appropriate aquaria.

Briefly, the *V. anguillarum* was inoculated in LB broth in a shaker (180 rpm) at 28 °C overnight. The fish were immersed at a final concentration of 5×10^7 CFU/mL for 2 h in bucket, while the control fish were immersed in sterilized media alone. Following immersion, the fish were transferred back in the flow-through system. Aquaria were randomly assigned for 2 h, 6 h, 12 h and 24 h post-treatment and 0 h control with 30 fish in each aquarium for sample collection.

The *S. iniae* isolate was inoculated in LB broth in a shaker incubator at 28 °C overnight. The fish were equally divided into 5 aquariums, 4 challenged groups and one control group with 30 fish in each group. For the challenge, the fish were immersed for 2 h at a final concentration of 5×10^6 CFU/mL in bucket, while the control fish were immersed in sterilized media alone. Following immersion, the fish were transferred back in the flow-through system. The samples were collected at 2 h, 4 h, 8 h and 12 h post challenge. All samples from both experiments were flash-frozen in liquid nitrogen and then stored in a −80 °C ultra-low freezer until preparation of RNA.

2.5. Total RNA extraction and cDNA synthesis

Prior to RNA extraction, tissue samples were homogenized under liquid nitrogen using mortar and pestle. Total RNA was extracted using Trizol® Reagent (Invitrogen, USA) according to the supplied protocol. The quality and quantity of RNA of each sample were measured on a Nanodrop 2000 (Thermo Electron North America LLC, FL). All extracted samples had an A260/280 ratio greater than 1.8.

2.6. Real-time PCR analysis

Gene specific primers for *Sm*Lgals4 were designed using Primer3 software based on the turbot galectin-3 sequences. And 18S rRNA gene was used as a reference gene (Table 1). First strand cDNA was synthesized by PrimeScript RT reagent Kit (TaKaRa) according to manufacturer's protocol (500 ng RNA per 10 μl reaction). Quantitative real-time PCR (qPCR) was performed on a CFX96 real-time PCR detection system (Bio-Rad Laboratories, Hercules, CA) using the SYBR ExScript qRT-PCR Kit (Takara, Dalian, China). The reaction systems for all real-time PCR were as follows: 1.0 μL of each primer (5 μM), 5.0 μL SYBR Green supermix, 2.0 μL RNase/DNase-free water, and 1.0 μl 200 ng/μL cDNA. The PCR reaction mixture was denatured at 95 °C for 30 s and then subjected to 40 cycles of 95 °C for 5 s, 58 °C for 5 s and followed by dissociation curve analysis, 5 s at 65 °C, then up to 95 °C at a rate of 0.1 °C/s increment, to verify the specificity of the amplicons. Results were analyzed using Relative Expression Software Tool (REST) to capture the significance at the level of $P < 0.05$ [31]. In order to determine the gene expression patterns in turbot healthy tissues, the tissue with the lowest Ct values was used as control. The mRNA expression levels of all samples were normalized to the levels of 18S ribosomal RNA gene in the same samples. A no-template control was run on all

Table 1
Primers used in this study.

Primer	Sequence (5′-3′)
qRT-PCR	
Sm-lgals4 F	5′GGATACCCCGGATCAAACCT3′
Sm-lgals4 R	5′ATCTGCTCGCCACAAAGTTG3′
18s RNA F	5′ATGGCCGTTCTTAGTTGGTG3′
18s RNA R	5′CTCAATCTCGTGTGGCTGAA3′
Protein expression	
Sm-lgals4-pr F	5′ATGACCTTTGTCGCTCCTCC3′
Sm-lgals4-pr R	5′TCAGAAGTGGATGTAGGAGATCTG3′

plates.

2.7. Plasmid construction

In order to construct the expression plasmid for *Sm*Lgals4, *Sm*Lgals4 was amplified with the specific primers following cDNA synthetization. The PCR products were ligated to pEASY-Blunt-E1 vector following gel extraction, and then transformed into competent Trans1-T1 cells. Following blue-white spotting selection, the positive clones were selected and sequencing with T7 Promoter Primer. The verified recombinant plasmid was extracted and marked as pEASY-E1- Lgals4.

2.8. Expression and purification of recombinant SmLgals4

The recombinant plasmid pEASY-E1- Lgals4 was transformed into *E. coli* BL21 (DE3). The transformant BL21- Lgals4 and the control BL21 with empty pET-32a were cultured in LB medium, and then induced by adding 0.5 mM isopropyl-b-D-thiogalactopyranoside. The expressed protein was purified by nickel-nitrilotriacetic acid chromatography, and analyzed by 12% sodium dodecyl sulfate polyacrylamide gel electrophoresis (SDS-PAGE) and visualized by staining with Coomassie brilliant blue. The concentration of the recombinant protein was determined using Bradford's method.

2.9. Solid-phase enzyme-linked immunosorbent assay (ELISA)

The binding ability of recombinant *Sm*Lgals4 (*rSm*Lgals4) with lipopolysaccharide (LPS), lipoteichoic acid (LTA) and peptidoglycan (PGN) was characterized by ELISA method. Briefly, LPS/LTA/PGN (5 μg/mL) were coated to 96 microtitor plate at 4 °C overnight. The wells were washed with 300 μl PBST three times, and blocked with 100 μl 5% BSA at 4 °C for 1 h. Then, 100 μl of the increasing concentrations of purified recombinant *Sm*Lgals4 (0.5, 1, 2, 4, and 8 μg/mL) were added into each ligand-coated well, with four replicates for each concentration, and incubated at 37 °C for 1 h. Subsequently, the wells were incubated at 37 °C for 1 h with 100 μl mouse anti-His antibody (Solarbio, Beijing, China) (diluted 1:1000 in 5% BSA), followed by another incubation at 37 °C for 40 min with the addition of 100 μl horseradish peroxidase conjugated goat anti-mouse IgG (Solarbio, Beijing, China) (diluted 1:1000 in 5% BSA). Finally, the reaction was terminated by adding 0.5M sulfate, and the plate was then read at 450 nm with an ELISA reader.

3. Results

3.1. Identification of turbot galectin-4 gene

In this study, one galectin-4 gene was identified in turbot (*Sm*Lgals4). In detail, the full-length *Sm*Lgals4 (GenBank accession: MH182625) transcript contains a 1197 bp open reading frame (ORF) encoding 398 amino acids residues with a predicted molecular mass of a 41.82 kDa and a theoretical isoelectric point of 5.3 (Table 2). The deduced *Sm*Lgals4 protein was predicted to have 1 Protein kinase C phosphorylation sites, 3 Casein kinase II phosphorylation sites, and 2 N-glycosylation sites (Table 2), as well as 32 negatively charged residues (Asp + Glu), 25 positively charged residues (Arg + Lys), and with an instability index of 46.11 and aliphatic index of 55.25 (Table 2). In comparison to other species, *Sm*Lgals4 showed the highest similarity to large yellow croaker (62%), followed by Mexican tetra (57.6%), while the highest identity was also observed with large yellow croaker (61.93%), followed by Mexican tetra (53.9%) (Table 3).

3.2. Genomic structure analysis of SmLgals4

Subsequently, the genomic architecture of *Sm*Lgals4 was investigated to compare the exon/intron organization across the vertebrates (Fig. 1). In general, the higher vertebrates had fewer number of exons (10 exons for human and mouse, 11 exons for tropical clawed frog), while the teleost had more number of exons (14 exons for half-smooth tongue sole and turbot, 15 exons for catfish and large yellow croaker) (Fig. 1). However, the same exons were observed in N-terminal and C-terminal across all the species. In detail, the first three exons (45 bp, 89 bp and 205 bp) were presented in N-terminal, while the last three exons (89 bp, 166 bp and 147 bp) were detected in C-terminal (Fig. 1).

Table 2
Primary structural analysis. Properties of turbot *Sm*Lgals4 gene determined by ProtParam.

Analysis	*Sm*Lgals4
No. of amino acids	398
Molecular weight (kDa)	41.82
Theoretical pI	5.3
Total number of negatively charged residues (Asp + Glu)	32
Total number of positively charged residues (Arg + Lys)	25
Formula	$C_{1835}H_{2768}N_{506}O_{549}S_{35}$
Instability index	46.11
Aliphatic index	55.25
Grand average of hydropathicity (GRAVY)	−0.206
Protein kinase C phosphorylation site	1
Casein kinase II phosphorylation site	3
N-glycosylation site	2

Table 3
Amino acid comparison of *Sm*Lgals4 gene with other species using MatGAT program.

Species	*Smgals4*	
	Similarity	Identity
Turbot *lgals4*		
Channel catfish *lgals4*	49.3	46,3
Human *lgals4*	50.7	48.1
Mouse *lgals4*	49.3	48.4
Mexican tetra *lgals4*	57.6	53.9
Large yellow croaker *lgals4*	62	61.9
Central bearded dragon *lgals4*	49.7	47.4
Tongue sole *lgals4*	44.5	41.8
Tropical clawed frog *lgals4*	49.9	49.1
Japanese medaka *lgals4*	43.5	43.3

3.3. Phylogenetic analysis

The phylogenetic analysis was then performed with amino acid sequences of galectin-4 from species of fish and mammals, using MEGA 6 with the neighbor-joining method. In our results, *Sm*Lgals4 was firstly clustered with large yellow croaker, and then clustered with half-smooth tongue sole and Japanese medaka, and formed clade with catfish and mexican tetra (Fig. 2). The higher vertebrates formed a single clade including human, mouse, central bearded dragon and bald eagle (Fig. 2). And all branching nodes were supported by high bootstrap values.

3.4. Syntenic analysis

The syntenic analysis was performed for further validation of the identification of *Sm*Lgals4. In general, a conserved synteny was detected among the selected species (Fig. 3). In detail, the turbot shared the same neighboring genes with human and mouse, including G-protein coupled receptor 4 (GPR4), Optic atrophy 3 protein homolog (OPA3), Ryanodine receptor 1 (RYR1), Transforming growth factor beta-1 (TGFB1), Serine/threonine-protein phosphatase 5 (PPP5C),

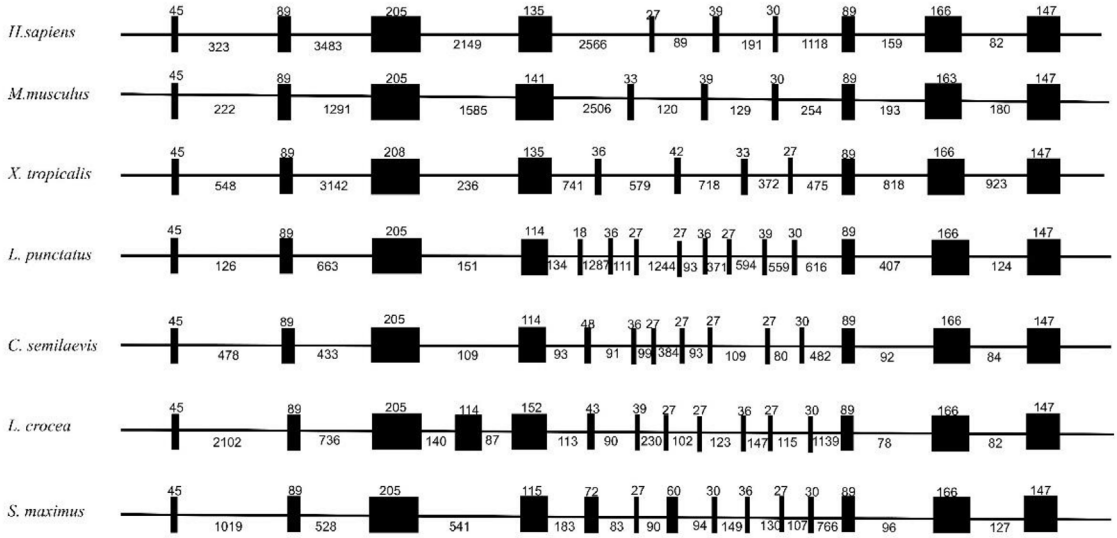

Fig. 1. Exon/intron organization of *Sm*Lgals4 gene was obtained by using Splign to align their cDNA sequences to the turbot genome. Boxes indicate exons and dashes indicate introns. The dark shaded boxes indicate exon sequences that encoding amino acids.

THAP domain-containing protein 8 (THAP8), and EH domain-containing protein 2 (EHD2), while few neighboring genes were missed comparing to medaka and half-smooth tongue sole (Fig. 3).

3.5. The tissue distribution of SmLgals4

The expression patterns of *Sm*Lgals4 were then investigated in eight turbot healthy tissues by real-time PCR method. In our results, the highest expression level of *Sm*Lgals4 was detected in intestine with 19.70 fold, followed by spleen with 3.51 fold, while the lowest expression level was observed in skin (Fig. 4). Actually, except the dramatically high expression level of *Sm*Lgals4 in intestine, there are no significant difference of the expression level of *Sm*Lgals4 in other tissues (Fig. 4).

3.6. Expression profiles of SmLgals4 following bacterial challenge

The expression profiles of *Sm*Lgals4 were examined in mucosal tissues (gill, skin and intestine) at early timepoints following immersion challenge with Gram-negative bacteria *V. anguillarum*, and Gram-positive bacteria *S. iniae*, respectively.

Following *V. anguillarum* challenge, *Sm*Lgals4 was only down-regulated in intestine, with the quickly down-regulation at 2 h with −10.79 fold, followed by −5.09 fold at 6 h, and returned to basal level at 12 h and 24 h (Fig. 5). In contrast, *Sm*Lgals4 was up-regulated in skin with 3.42 fold at 6 h, and 4.35 fold at 12 h, while no significant changes were observed in gill (Fig. 5).

In *S. iniae* challenge, similar to *V. anguillarum* challenge, the only down-regulation of *Sm*Lgals4 was also detected in intestine at all the timepoints following challenge, with −4.76 fold at 2 h, −3.33 fold at 4 h, −6.56 fold at 8 h, and −8.43 fold at 12 h (Fig. 6). However, similar to *V. anguillarum* challeng, the only up-regulation of *Sm*Lgals4 was observed in gill with 2.77 fold at 8 h and 3.76 fold at 12 h, while no significant changes were observed in skin (Fig. 6).

3.7. Microbial ligand-binding in vitro

Finally, the binding ability of *Sm*Lgals4 was investigated to further characterize its immune function. In detail, the *rSm*Lgals4 was purified from *E. coli* as a native His-tagged protein. In SDS-PAGE analysis, only a single band was observed (Supplementary Fig.1). In *in vitro* bingding assay analysis, *rSm*Lgals4 showed the strongest binding ability to LPS, followed by PGN and LTA (Fig. 7). In detail, the binding ability of *rSm*Lgals4 to LPS was higher than PGN at each concentration, and the highest binding ability of *rSm*Lgals4 to LTA at 8 μg/mL was lower than that to LPS and PGN at 0.5 μg/mL (Fig. 7).

4. Discussion

Cell surface glycans could modulates the interactions between cells and the extracellular matrix, by specifically regulating the binding to carbohydrate-binding receptors. The lectins are featured to form lectin-carbohydrate interactions with foreign pathogens through their CRDs by binding to glycans on the cell surface [6,32]. Among the different

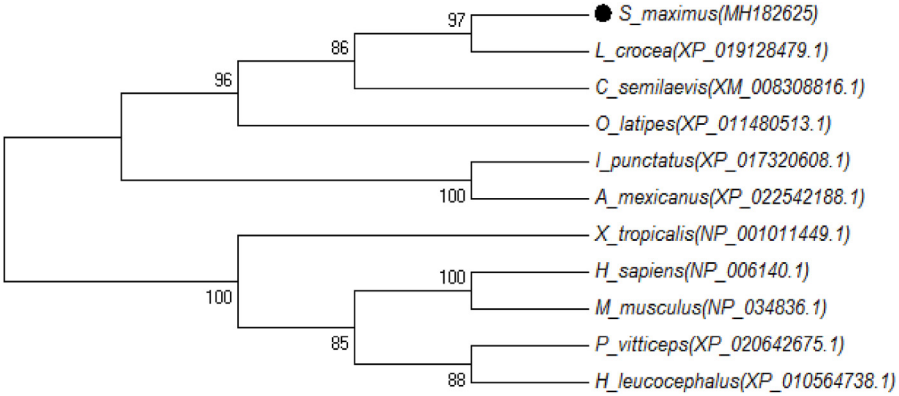

Fig. 2. Phylogenetic tree for the *Sm*Lgals4 gene. The phylogenetic tree was constructed based on the amino acid sequences of *Sm*Lgals4 from different species using the neighbor-joining method in MEGA 6. Gaps were removed by complete deletion and the phylogenetic tree was evaluated with 1000 bootstrap replications. The bootstrapping values were indicated by numbers at the nodes. Dark solid circles indicated the newly characterized *Sm*Lgals4 gene.

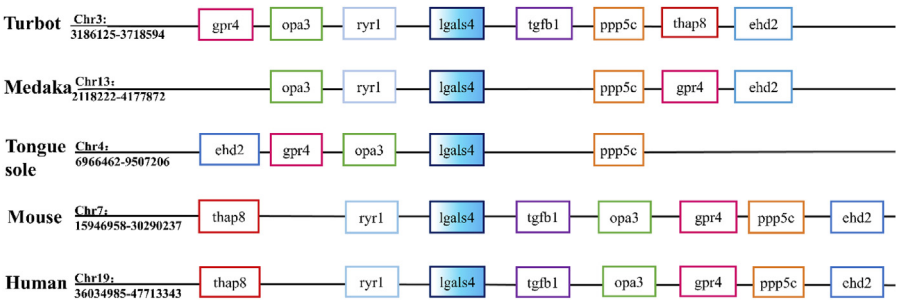

Fig. 3. Syntenic analysis of *SmLgals4* gene from different species. The Lgals4 gene is highlighted by bright blue color filled boxes. GPR4: G-protein coupled receptor 4; 0PA3: Optic atrophy 3 protein homolog; RYR1: Ryanodine receptor 1; TGFB1: Transforming growth factor beta-1; PPP5C: Serine/threonine-protein phosphatase 5; THAP8: THAP domain-containing protein 8; EHD2: EH domain-containing protein 2. (For interpretation of the references to color in this figure legend, the reader is referred to the Web version of this article.)

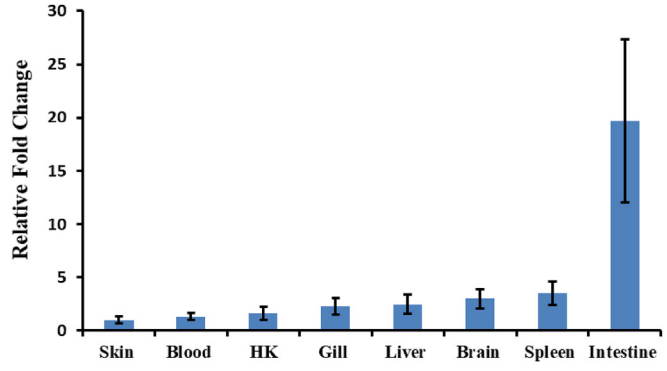

Fig. 4. The tissue distribution of *Sm*Lgals4 in turbot. *Sm*Lgals4 expression in liver, skin, spleen, blood, head kidney, intestine, gill and brain was determined by quantitative real-time PCR. The expression level of *Sm*Lgals4 in skin was set as 1. The relative abundance of *Sm*Lgals4 was expressed as mean ± SE (N = 3).

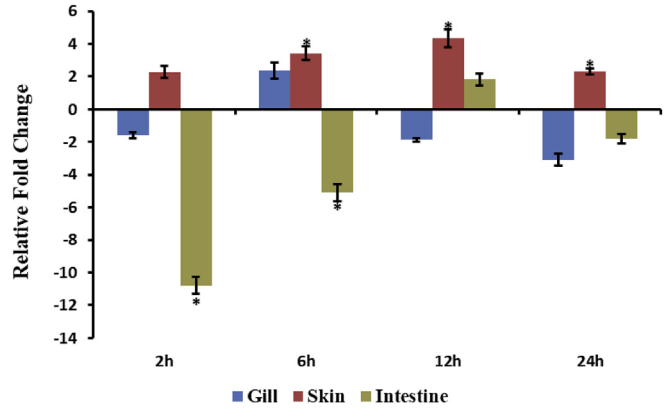

Fig. 5. The expression patterns of *Sm*Lgals4 in turbot tissues at different timepoints (2 h, 6 h, 12 h, and 24 h) after *V. anguillarum* challenge. *Sm*Lgals4 expression in skin, intestine and gill was determined by quantitative real-time PCR. 18S rRNA was employed as an internal control. Asterisks (*) marked the significant differences between experimental and control groups ($P < 0.05$). Error bars indicated standard error (n = 3).

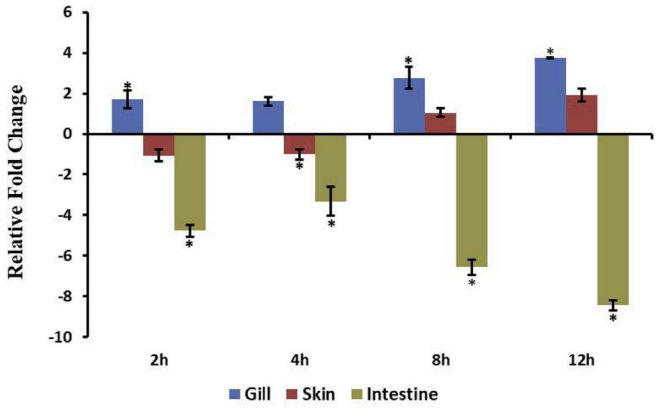

Fig. 6. The expression patterns of *Sm*Lgals4 in turbot mucosal tissues at different timepoints (2 h, 4 h, 8 h, and 12 h) after *S. iniae* challenge. *Sm*Lgals4 expression in skin, intestine and gill was determined by quantitative real-time PCR. 18S rRNA was employed as an internal control. Asterisks (*) marked the significant differences between experimental and control groups ($P < 0.05$). Error bars indicated standard error (n = 3).

lectin families, galectin have been shown to play vital roles in different levels of immune response in both vertebrates and invertebrates [15,33,34]. Although numerous studies have documented the function of galectin genes in mammals, only few studies have characterized the galectin genes in teleost. These include galectin-8 in tilapia [35], galectin-1 in flounder, sea bass and Atlantic cod [36–38], galectin-4 in snakehead [15], galectin-9 in large yellow croaker [34], and 12 galectin genes in catfish [33]. Among the galectin members, galectin-4 is discovered in intestine and has been revealed to play vital roles in mucosal immunity in mammals [12,13]. Accordingly, we here identified galectin-4 gene in turbot, investigated its immune roles in response to different bacterial infection in mucosal immunity, as well as the binding ability to different microbial ligands, to gain initial insight into the immune roles of galectin-4 in teleost mucosal immunity. In current study, we identified one galectin-4 gene in turbot (*Sm*Lgals4) with similar molecular properties to other fish species (Table 1). As an evolutionarily highly conserved family of proteins, the genomic structure analysis, phylogenetic analysis and syntenic analysis validated the identification of *Sm*Lgals4 and showed the strong orthology to their counterparts in vertebrate species.

In tissue distribution analysis, although *Sm*Lgals4 was widely expressed in all the examined tissues, it showed dramatically high expression level in intestine compared to all the other examined tissues (Fig. 4). As a soluble lectin originally discovered in rat intestine [10], galectin-4 has been shown to predominantly expressed in intestine, as well as in other tissues including kidney, liver, and spleen [39]. In contrast, galectin-4 showed high expression levels in liver, kidney and spleen, while lowly expressed in intestine, skin and gill of sneakhead [15]. Additionally, it was abundantly expressed in adult liver, kidney, digestive tract and whole embryos in *Xenopus laevis* [40]. With the limited information of tissue distribution patterns of galectin-4 in teleost, these differences might suggest galectin-4 plays different roles in different species.

The expression profiles of *Sm*Lgals4 were then characterized in turbot mucosal surfaces (skin, gill and intestine) following different bacteria challenge by immersion. The greatest interest is that *Sm*Lgals4 showed dramatic down-regulation in intestine in both Gram-negative bacteria *V. anguillarum*, and Gram-positive bacteria *S. iniae* challenge. In turbot, intestine has been long considered as a portal of entry for *V. anguillarum* [41], *V. anguillarum* cells could be detected in spleens in more than 50% of orally infected fish [42]. Moreover, *V. anguillarum* showed strong ability to survive in the acidic environment of the turbot stomach, and proliferated in the intestine quickly [43]. In rainbow trout

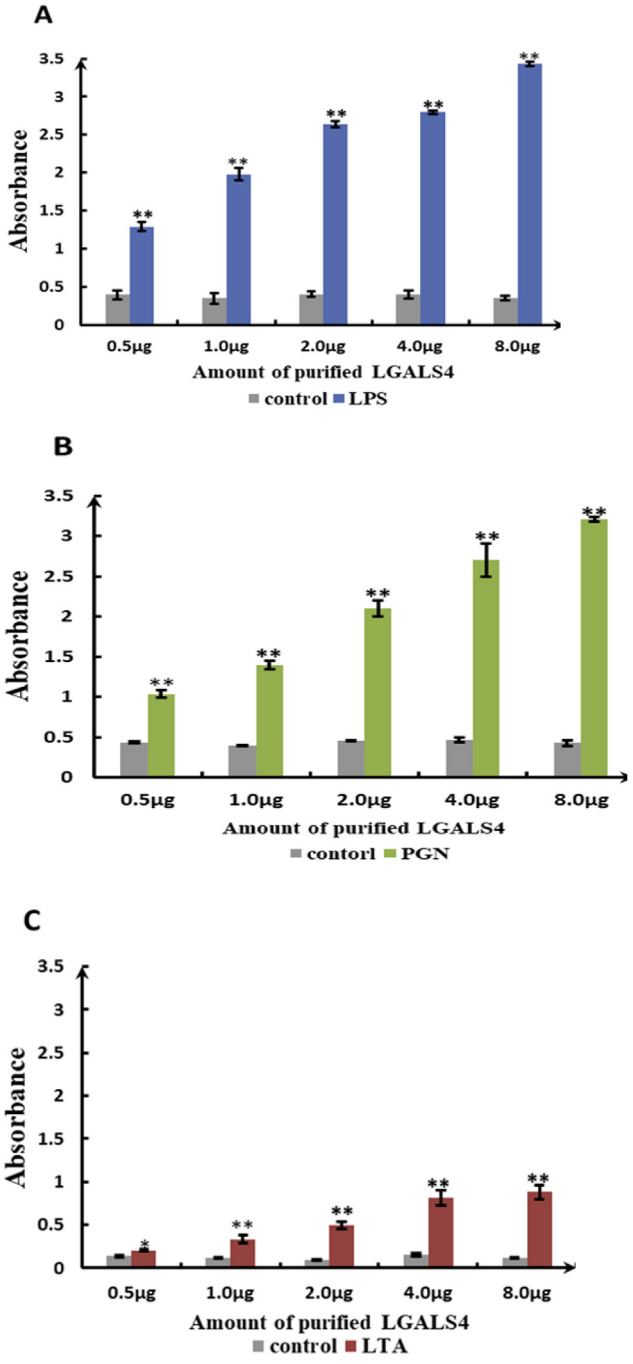

Fig. 7. Results of the *in vitro* binding assay of *Sm*Lgals4 on microbial ligands, including lipopolysaccharide, peptidoglycan, and lipoteichoic acid. * indicate a significant difference in the absorbance between different microbial ligands that exposed to *rSm*Lgals4 and the control group: *p < 0.05; **p < 0.01.

(*Oncorhynchus mykiss*), *V. anguillarum* was more chemotactic to intestinal mucus than gill mucus [44,45]. In zebrafish, *V. anguillarum* was firstly detected in intestine following immersion challenge [46]. Additionally, following bath-vaccination of live attenuated *V. anguillarum* vaccine, the bacteria was detected in intestine as early as 3 h, and persisted in the intestine for a longer time whereas decreased rapidly in the skin and gills [47]. Similar to *V. anguillarum* challenge, *Sm*Lgals4 was significantly down-regulated in all the timepoints in the intestine following *S. iniae* challenge. In Japanese flounder, the deaths were observed even at the lowest inoculation dose following *S. iniae* bath challenge [48]. Similarly, several immune-related genes showed significant up-regulation following *S. iniae* infection in turbot intestine [18–20]. Here, the significant down-regulation of galectin-4 in turbot intestine following different bacteria challenge suggested its vital roles in intestinal immune responses. Further work is warranted to examine whether turbot galectin-4 may play similar roles in intestine as mammals.

In intestinal barrier, galectin-4 have been considered to mediating lateral cell interactions between intestinal epithelial cells to increase the barrier integrity [49]. And galectin-4 was demonstrated to be secreted from both basolateral and apical sides of the intestinal epithelial cells [50]. In the impaired intestinal epithelial barrier, galectin-4 was found to promote the cell migration and proliferation, then enhance the epithelial cell moving to damaged area for healing through a TGF-beta-independent mechanism [12]. Although galectin-4 showed strong bactericidal activity in teleost, it was also reported to induce the intestinal inflammation in inflammatory bowel disease, the administration of galectin-4 antibody into mice could significantly suppress the intestinal inflammation [14]. In our results, *Sm*Lgals4 was dramatically down-regulated in the intestine in both *V. anguillarum* and *S. iniae* challenge, which might suggested the suppressed intestinal inflammation in turbot intestine, and also indicated the pro-inflammation role of galectin-4 in teleost. This information has been added in the manuscript. Finally, r*Sm*Lgals4 showed strong binding ability to LPS and PGN, followed by LTA. As a member of PRRs, galectins possessed carbohydrate binding ability to microbial pathogens by recognizing exogenous ligands, especially carbohydrates on the surface of microbes via their CRDs, and subsequently trigger downstream immune signaling pathways to eliminate the pathogens. Although the key roles of galectin-4 in intestinal epithelial barrier have been well recognized, the detailed roles of galectin-4 in teleost are still lacking, further studies are needed to be carried out to characterize whether plays similar roles in teleost intestinal immunity.

Acknowledgement

This study was supported by the National Science Foundation of China (No.:31602193). It was also supported by keypoint research and invention program in Shandong Province (2017GHY215004), and the fish innovation team of Shandong Agriculture Research System (SDAIT-12-05).

Appendix A. Supplementary data

Supplementary data to this article can be found online at https://doi.org/10.1016/j.fsi.2018.10.050.

References

[1] A. Foey, S. Picchietti, Immune Defences of Teleost Fish, John Wiley & Sons, Ltd, 2014.
[2] Y. Kumagai, O. Takeuchi, S. Akira, Pathogen recognition by innate receptors, J. Infect. Chemother. 14 (2) (2008) 86–92.
[3] L.Y. Zhu, L. Nie, G. Zhu, L.X. Xiang, J.Z. Shao, Advances in research of fish immune-relevant genes: a comparative overview of innate and adaptive immunity in teleosts, Dev. Comp. Immunol. 39 (1–2) (2013) 39.
[4] O. Tomohisa, W. Mizuki, N. Takako, M. Koji, Diversified carbohydrate-binding lectins from marine resources, J. Amino Acids (2011) (2011-11-15) 2011(1) (2011) 838914.
[5] G.R. Vasta, M. Nita-Lazar, B. Giomarelli, H. Ahmed, S. Du, M. Cammarata, N. Parrinello, M.A. Bianchet, L.M. Amzel, Structural and functional diversity of the lectin repertoire in teleost fish: relevance to innate and adaptive immunity, Dev. Comp. Immunol. 35 (12) (2011) 1388.
[6] G.R. Vasta, H. Ahmed, S.J. Du, D. Henrikson, Galectins in teleost fish: zebrafish (Danio rerio) as a model species to address their biological roles in development and innate immunity, Glycoconj. J. 21 (8–9) (2004) 503–521.
[7] D.K. Hsu, R.Y. Yang, F.T. Liu, Galectins in apoptosis, Methods Enzymol. 417 (2006) 256.
[8] J. Hirabayashi, K. Kasai, The family of metazoan metal-independent beta-galactoside-binding lectins: structure, function and molecular evolution, Glycobiology 3 (4) (1993) 297–304.
[9] R.Y. Yang, G.A. Rabinovich, F.T. Liu, Galectins: structure, function and therapeutic

potential, Expet Rev. Mol. Med. 10 (article e17) (2015) e17.
[10] H. Leffler, F.R. Masiarz, S.H. Barondes, Soluble lactose-binding vertebrate lectins: a growing family, Biochemistry 28 (23) (1989) 9222–9229.
[11] E. Niepceron, F. Simian, P. Louisot, M.C. Bioln'Garagba, Expression of galectin 4 in the rat small intestine during postnatal development, Biochimie 86 (2) (2004) 115–118.
[12] D. Paclik, K. Lohse, B. Wiedenmann, A.U. Dignass, A. Sturm, Galectin-2 and -4, but not galectin-1, promote intestinal epithelial wound healing in vitro through a TGF-beta-independent mechanism, Inflamm. Bowel Dis. 17 (6) (2011) 1366–1372.
[13] D. Paclik, S. Danese, U. Berndt, B. Wiedenmann, A. Dignass, A. Sturm, Galectin-4 controls intestinal inflammation by selective regulation of peripheral and mucosal T cell apoptosis and cell cycle, PloS One 3 (7) (2008) e2629.
[14] A. Hokama, E. Mizoguchi, K. Sugimoto, Y. Shimomura, Y. Tanaka, M. Yoshida, S.T. Rietdijk, Y.P.D. Jong, S.B. Snapper, C. Terhorst, Induced reactivity of intestinal CD4 + T cells with an epithelial cell lectin, galectin-4, contributes to exacerbation of intestinal inflammation, Immunity 20 (6) (2004) 681–693.
[15] A. Arasu, V. Kumaresan, M.R. Ganesh, M. Pasupuleti, M.V. Arasu, N.A. Al-Dhabi, J. Arockiaraj, Bactericidal activity of fish galectin 4 derived membrane-binding peptide tagged with oligotryptophan, Dev. Comp. Immunol. 71 (2017).
[16] I. Salinas, The mucosal immune system of teleost fish, Biology 4 (2015).
[17] S.P. Biswas, A.G. Jadhao, R.C. Bhoyar, N.V. Palande, D.P. Sinh, Neuroanatomical localization of nitric oxide synthase (nNOS) in the central nervous system of carp, Labeo rohita during post-embryonic development, Int. J. Dev. Neurosci. 46 (2015) 14–26.
[18] L. Zhang, C. Gao, F. Liu, L. Song, B. Su, C. Li, Characterization and expression analysis of a peptidoglycan recognition protein gene, SmPGRP2 in mucosal tissues of turbot (Scophthalmus maximus L.) following bacterial challenge, Fish Shellfish Immunol. 56 (2016) 367.
[19] X. Dong, B. Su, S. Zhou, M. Shang, H. Yan, F. Liu, C. Gao, F. Tan, C. Li, Identification and expression analysis of toll-like receptor genes (TLR8 and TLR9) in mucosal tissues of turbot (Scophthalmus maximus L.) following bacterial challenge, Fish Shellfish Immunol. 58 (2016) 309–317.
[20] X. Dong, Q. Fu, S. Liu, C. Gao, B. Su, F. Tan, C. Li, The expression signatures of neuronal nitric oxide synthase (NOS1) in turbot (Scophthalmus maximus L.) mucosal surfaces against bacterial challenge, Fish Shellfish Immunol. 59 (2016) 406–413.
[21] C. Gao, Q. Fu, S. Zhou, S. Lin, Y. Ren, X. Dong, B. Su, C. Li, The mucosal expression signatures of g-type lysozyme in turbot (Scophthalmus maximus) following bacterial challenge, Fish Shellfish Immunol. 54 (2016) 612.
[22] F. Liu, B. Su, C. Gao, S. Zhou, L. Song, F. Tan, X. Dong, Y. Ren, C. Li, Identification and expression analysis of TLR2 in mucosal tissues of turbot (Scophthalmus maximus L.) following bacterial challenge, Fish Shellfish Immunol. 55 (2016) 654.
[23] C. Gao, F. Qiang, B. Su, S. Zhou, F. Liu, S. Lin, Z. Min, Y. Ren, X. Dong, F. Tan, Transcriptomic profiling revealed the signatures of intestinal barrier alteration and pathogen entry in turbot (Scophthalmus maximus) following Vibrio anguillarum challenge, Dev. Comp. Immunol. 65 (2016) 159–168.
[24] F. Antonio, R. Diego, C. André, H. Miguel, P. Patricia, J.A. Rubiolo, G.G. Jèssica, C. Laia, B. Xabier, G. Marta, Whole genome sequencing of turbot (Scophthalmus maximus; Pleuronectiformes): a fish adapted to demersal life, DNA Res. 23 (3) (2016) 181–192 2016-3-6) 23(3.
[25] M.R. Wilkins, E. Gasteiger, A. Bairoch, J.C. Sanchez, K.L. Williams, R.D. Appel, D.F. Hochstrasser, Protein identification and analysis tools in the ExPASy server, Methods Mol. Biol. 112 (112) (1999) 571–607.
[26] Y. Kapustin, A. Souvorov, T. Tatusova, D. Lipman, Splign: algorithms for computing spliced alignments with identification of paralogs, Biol. Direct 3 (1) (2008) 20.
[27] J.J. Campanella, L. Bitincka, J. Smalley, MatGAT, An application that generates similarity/identity matrices using protein or DNA sequences, BMC Bioinf. 4 (1) (2003) 29.
[28] F. Sievers, A. Wilm, D. Dineen, T.J. Gibson, K. Karplus, W. Li, R. Lopez, H. Mcwilliam, M. Remmert, J. Söding, Sievers F, Wilm A, Dineen D, Gibson TJ, Karplus K, Li W et al.. Fast, scalable generation of high-quality protein multiple sequence alignments using Clustal Omega. Mol. Syst. Biol. 7: 539, Molecular Systems Biology 7(1) (2011) 539.
[29] K. Tamura, G. Stecher, D. Peterson, A. Filipski, S. Kumar, MEGA6: molecular evolutionary Genetics analysis version 6.0, Mol. Biol. Evol. 30 (12) (2013) 2725.
[30] M. Muffato, A. Louis, C.E. Poisnel, H.R. Crollius, Genomicus, Bioinformatics 26 (8) (2010).
[31] M.W. Pfaffl, G.W. Horgan, L. Dempfle, Relative expression software tool (REST) for group-wise comparison and statistical analysis of relative expression results in real-time PCR, Nucleic Acids Res. 30 (9) (2002) e36-e36(1).
[32] G.R. Vasta, Galectins as pattern recognition receptors: structure, function, and evolution, Oxygen Transport to Tissue XXXIII 946 (946) (2012) 21–36.
[33] S. Zhou, H. Zhao, W. Thongda, D. Zhang, B. Su, Y. Dan, E. Peatman, L. Chao, Galectins in channel catfish, Ictalurus punctatus : characterization and expression profiling in mucosal tissues, Fish Shellfish Immunol. 49 (2016) 324–335.
[34] D.L. Zhang, C.H. Lv, D.H. Yu, Z.Y. Wang, Characterization and functional analysis of a tandem-repeat galectin-9 in large yellow croaker Larimichthys crocea, Fish Shellfish Immunol. 52 (2016) 167–178.
[35] S. Unajak, N. Pholmanee, N. Songtawee, K. Srikulnath, P. Srisapoome, A. Kiataramkul, H. Kondo, I. Hirono, N. Areechon, Molecular characterization of Galectin-8 from Nile tilapia (Oreochromis niloticus Linn.) and its response to bacterial infection, Mol. Immunol. 68 (2) (2015) 585–596.
[36] S. Liu, G. Hu, C. Sun, S. Zhang, Anti-viral activity of galectin-1 from flounder Paralichthys olivaceus, Fish Shellfish Immunol. 34 (6) (2013) 1463–1469.
[37] L. Poisa-Beiro, S. Dios, H. Ahmed, G.R. Vasta, A. Martínez-López, A. Estepa, J. Alonso-Gutiérrez, A. Figueras, B. Novoa, Nodavirus infection of sea bass (Dicentrarchus labrax) induces up-regulation of galectin-1 expression with potential anti-inflammatory activity, J. Immunol. 183 (10) (2009) 6600.
[38] B. Rajan, V. Kiron, J.M. Fernandes, M.F. Brinchmann, Localization and functional properties of two galectin-1 proteins in Atlantic cod (Gadus morhua) mucosal tissues, Dev. Comp. Immunol. 40 (2) (2013) 83–93.
[39] Y. Oda, J. Herrmann, M.A. Gitt, C.W. Turck, A.L. Burlingame, S.H. Barondes, H. Leffler, Soluble lactose-binding lectin from rat intestine with two different carbohydrate-binding domains in the same peptide chain, J. Biol. Chem. 268 (8) (1993) 5929–5939.
[40] H. Shoji, N. Nishi, M. Hirashima, T. Nakamura, Purification and cDNA cloning of Xenopus liver galectins and their expression, Glycobiology 12 (3) (2002) 163.
[41] J.C. Oisson, A. Jöborn, A. Westerdahl, L. Blomberg, S. Kjelleberg, P.L. Conway, Is the turbot, Scophthalmus maximus (L.), intestine a portal of entry for the fish pathogen Vibrio anguillarum? J. Fish. Dis. 19 (3) (1996) 225–234.
[42] J.C. Oisson, A. Jöborn, A. Westerdahl, L. Blomberg, S. Kjelleberg, P.L. Conway, Is the turbot, Scophthalmus maximus (L.), intestine a portal of entry for the fish pathogen Vibrio anguillarum? J. Fish. Dis. 19 (3) (2010) 225–234.
[43] Jöborn Olsson, Blomberg Westerdahl, Conway Kjelleberg, Survival, persistence and proliferation of Vibrio anguillarum in juvenile turbot, Scophthalmus maximus (L.), intestine and faeces, J. Fish. Dis. 21 (1) (2010) 1–9.
[44] M.H. Larsen, J.L. Larsen, J.E. Olsen, Chemotaxis of Vibrio anguillarum to fish mucus: role of the origin of the fish mucus, the fish species and the serogroup of the pathogen, FEMS Microbiol. Ecol. 38 (1) (2001) 77–80.
[45] R. O'Toole, S. Lundberg, S.Å. Fredriksson, A. Jansson, N. Bo, H. Wolf-Watz, The chemotactic response of Vibrio anguillarum to fish intestinal mucus is mediated by a combination of multiple mucus components, J. Bacteriol. 181 (14) (1999) 4308–4317.
[46] R. O'Toole, H.J. Von, R. Rosqvist, P.E. Olsson, H. Wolfwatz, Visualisation of zebrafish infection by GFP-labelled Vibrio anguillarum, Microb. Pathog. 37 (1) (2004) 41–46.
[47] X. Liu, H. Wu, X. Chang, Y. Tang, Q. Liu, Y. Zhang, Notable mucosal immune responses induced in the intestine of zebrafish (Danio rerio) bath-vaccinated with a live attenuated Vibrio anguillarum vaccine, Fish Shellfish Immunol. 40 (1) (2014) 99–108.
[48] N.H. Thinh, Immunohistochemical examination of experimental Streptococcus iniae infection in Japanese flounder Paralichthys olivaceus, Fish Pathol. 36 (3) (2009) 40–41.
[49] D.N. Cooper, Galectinomics: finding themes in complexity, Biochim. Biophys. Acta Gen. Subj. 1572 (3) (2002) 209–231.
[50] A. Hokama, E. Mizoguchi, A. Mizoguchi, Roles of galectins in inflammatory bowel disease, World J. Gastroenterol. 14 (33) (2008) 5133–5137.